Fundamental Properties of Inert Gas Mixtures for Plasma Display Panels

Georgios Veronis, Umran S. Inan, *Senior Member, IEEE*, and Victor P. Pasko

***Abstract*—A fundamental kinetic model is used to compare the luminous efficiency of different compositions of Ne–Xe, He–Xe, and Ne–Xe–Ar mixtures in plasma display panels. A self-sustaining condition is used to estimate the breakdown electric field E_k, accounting also for Penning ionization. The excitation frequency of Xe states that emit UV photons is calculated for applied electric field values ranging from $0.2E_k$ to $5E_k$. Light generation efficiency, defined as the ratio of the energy spent in excitation of UV emitting states of Xe per unit volume and per unit time versus dissipated electrical power, is an increasing function of the Xe concentration $N_{\rm Xe}$ in both the Ne–Xe and He–Xe cases, although He–Xe mixtures were found to be somewhat less efficient. The fractional increase in efficiency is very small for $N_{\rm Xe} > 0.1N$. The addition of small amounts of Ar in Ne–Xe mixtures leads to insignificant changes in efficiency or breakdown voltage level. Results of a one-dimensional (1-D) self-consistent simulation of an ac plasma display cell are consistent with the conclusions derived based on the homogeneous unbounded kinetic analysis.**

***Index Terms*—Gas discharge, plasma display panel (PDP), Xe.**

I. Introduction

PLASMA display panels (PDPs) are one of the leading candidates in the competition for large-size, high-brightness flat panel displays, suitable for high-definition television (HDTV) monitors [1], [2]. Their advantages are high resolution, fast response, wide viewing angle, low weight, and simple manufacturing process for fabrication. The fact that they are expected to be the next generation of TV displays is evident in the remarkable recent progress of PDP technology development and manufacturing [3], [4].

One of the most critical issues in PDP research and technology development is the improvement of luminance and luminous efficiency [1], which is dependent on the gas mixture composition, phosphor efficiency, driving voltage characteristics, and cell geometry. PDP cells can operate only if the applied voltage is held within certain limits. The minimum and maximum values of the applied voltage define the margin of the panel [5]. These limits are determined by the breakdown voltage. In some PDP designs, reducing the breakdown voltage may be of higher priority than is increasing the efficiency, because of the high cost of high-voltage driving circuits [1]. In this article, we focus our attention on the effects of gas mixture composition on light generation efficiency and on the breakdown voltage.

Manuscript received October 29, 1999; revised March 14, 2000. This work was supported by the National Science Foundation under Grant ATM-9731170.

The authors are with the Space, Telecommunications, and Radioscience Laboratory, Department of Electrical Engineering, Stanford University, Stanford, CA 94305-9515 USA (e-mail: inan@nova.stanford.edu).

Publisher Item Identifier S 0093-3813(00)07374-4.

Typical plasma displays consist of two glass plates, each with parallel electrodes deposited on their surfaces. The electrodes are covered with a dielectric film. The plates are sealed together with their electrodes at right angles, and the gap between the plates is filled with an inert gas mixture. A protective MgO layer is deposited above the dielectric film. The role of this layer is to decrease the breakdown voltage caused by the high secondary electron emission coefficient of MgO. The discharge is initiated by applying a voltage pulse to the electrodes. Xenon gas mixtures are used to efficiently generate UV photons. The UV photons emitted by the discharge hit the phosphors deposited on the walls of the PDP cell and are converted into visible photons. Each cell contains phosphor that emits one primary color—red, green, or blue.

In this paper, we study different Xenon gas mixtures and theoretically investigate their efficiency in generating UV photons. In particular, we examine three different cases, i.e., Ne–Xe, He–Xe, and Ne–Xe–Ar. In each case, we investigate the effect of the variation of the percentage of the constituent gases on the efficiency of the mixture and on the breakdown voltage. In Section II, we describe our approach, based on the fundamental processes that determine the gas mixture efficiency. In Section III, we present the results of our model. In Section IV, a one-dimensional (1-D) self-consistent simulation is used to assess the validity of the conclusions derived from the homogeneous and unbounded kinetic model. Our conclusions are summarized in Section V.

II. Formulation

In this work, we investigate the effect of the gas mixture on PDP performance from the point of view of the fundamental inherent properties of the constituent gases. For this purpose, we rely on exact numerical solutions of the kinetic Boltzmann equation in a homogeneous, unbounded system while accurately accounting for all the known processes of excitation as well as ionization and other losses. Our chosen measure of comparison of different mixtures is the efficiency η, defined as the ratio of the energy spent in excitation of UV emitting states of Xe per unit volume and per unit time, over the dissipated power per unit volume.

The luminous efficiency of a PDP cell is a measure of the number of photons emitted per unit power dissipated in the discharge. In color PDPs, the purpose of the discharge is to produce UV photons that are then converted to visible light by means of phosphors. UV photons that excite the phosphors and produce visible light [6] are emitted by certain excited states of Xe [$Xe^*(^3P_1)$ (resonant state) at 147 nm, $Xe_2^*(O_u^+)$ at 150 nm,

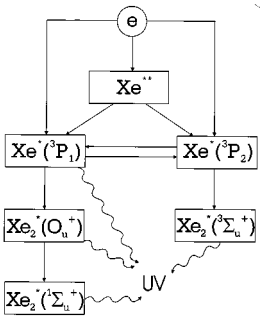

Fig. 1. Block diagram of reaction channels related to UV emitting excited states of Xe.

and $Xe_2^*(^3\Sigma_u^+)$ and $Xe_2^*(^1\Sigma_u^+)$ at 173 nm (excimer states)]. Although the duration of the discharge current pulse is on the order of 10 ns, emission of UV photons lasts for about 5 μs because of the lifetimes of some of the excited species [6]. Some excited states of Ne also radiate photons [7] [$Ne^*(^1P_1)$ at 736 Å, $Ne^*(^3P_1)$ at 743 Å], but these are not in the UV range and the visible orange glow actually deteriorates color purity [8]. Shown in Fig. 1 is a block diagram of reaction channels related to the excited states of Xe that produce UV photons [6]. Atoms in the $Xe^*(^3P_1)$, $Xe^*(^3P_2)$ (metastable), and Xe** (sum of the $6s'$, $6p$, $5d$, $7s$ states) excited states are mainly produced by electron impact excitation reactions. Because stepwise ionization is negligible and no other important loss mechanisms exist, all of the energy going into these excited states leads to the production of UV photons [6]. As a result, for a given gas mixture, the number of UV photons emitted by excited Xe atoms per electron in the discharge is determined by the excitation frequency ν_{exc} of the $Xe^*(^3P_1)$, $Xe^*(^3P_2)$, and Xe** excited states as a function of the reduced electric field E/N, where E is the electric field and N is the gas density. The energy spent on excitation of UV emitting states of Xe per unit volume and per unit time is

$$P_{\rm UV} = \nu_{exc} N_e \varepsilon_{\rm UV}$$

where N_e is the electron number density and $\varepsilon_{\rm UV}$ is the energy of an emitted UV photon, equal to the energy spent on the excitation of a Xe atom. (We consider 150-nm photons and do not take into account the frequency distribution of UV radiation, so that $\varepsilon_{\rm UV} \simeq 8.3$ eV). Although some UV emitting excited states of Xe have relatively long lifetimes, all of the energy spent on excitation of UV emitting states of Xe is eventually converted to UV photons. For our purposes, we can thus consider the efficiency η to be equal to the luminous efficiency.

The power dissipated in the discharge is determined by the voltage applied to the electrodes of the PDP cell and the discharge current. The driving voltage is related to the breakdown voltage, which depends on the gas mixture used. The dissipated power per unit volume caused by electron current is

$$P_{diss} = EJ_e = N_e q_e \mu_e E^2$$

where

J_e electron current density;
q_e electronic charge;
μ_e electron mobility.

Thus, the luminous efficiency is given as

$$\eta = \frac{\nu_{exc}\varepsilon_{\rm UV}}{q_e \mu_e E^2} = 8.3\left[\frac{\nu_{exc}}{\mu_e E^2}\right]. \quad (1)$$

Both of the quantities ν_{exc} and μ_e in (1) exhibit highly nonlinear dependence on the electric field E, so that the luminous efficiency can only be evaluated numerically. In this paper, we determine η by numerically solving the full electron Boltzmann equation to compare the efficiency of different gas mixtures by calculating the breakdown voltage and excitation of Xe states that lead to the production of UV photons. It should be noted that η, as defined in (1), represents the efficiency of the electrons in exciting UV emitting states of Xe. In an actual PDP cell, a fraction of the input energy is dissipated by the ions. However, (1-D) self-consistent calculations (Section IV) indicate that the dependence of the actual discharge efficiency on gas mixture composition is nevertheless well represented by η.

A. Ne–Xe Mixtures

For our homogeneous and unbounded system, we use a breakdown voltage equivalent to that which would result in a self-sustaining condition in a 1-D parallel plate geometry, with plate separation $d = 100$ μm, corresponding to the gap length of a typical PDP cell. This assumption is appropriate because the actual voltage that must be applied to the electrodes of the PDP cell to cause breakdown in the gas is directly proportional to the voltage obtained from the self-sustaining condition. In the Ne–Xe mixture case, this condition can be written as [9], [10]

$$\frac{\alpha_{\rm Ne}\gamma_{\rm Ne} + (\alpha_{\rm Xe} + \alpha_P)\gamma_{\rm Xe}}{\alpha_{\rm Ne} + \alpha_{\rm Xe} + \alpha_P}\left[e^{(\alpha_{\rm Ne}+\alpha_{\rm Xe}+\alpha_P)d} - 1\right] = 1 \quad (2)$$

where $\alpha_{\rm Ne} = \nu_{\rm Ne}/v_d$ and $\alpha_{\rm Xe} = \nu_{\rm Xe}/v_d$ are the partial first Townsend ionization coefficients for Ne and Xe, respectively, $\nu_{\rm Ne}$ and $\nu_{\rm Xe}$ are the corresponding partial ionization frequencies caused by direct ionization of neutral atoms by electrons, v_d is the electron drift velocity, and $\gamma_{\rm Ne}$ and $\gamma_{\rm Xe}$ are, respectively, the secondary electron emission coefficients for Ne and Xe ions impingent on MgO. The quantity α_P is the effective partial first Townsend ionization coefficient per electron caused by ionization by metastable neon atoms (Penning ionization). Neon metastable atoms have a much longer lifetime than do the other excited states of Ne and have an energy of $\varepsilon_{\rm m} \simeq 16.6$ eV. Thus, they are capable of ionizing the atoms of other gases having an ionization energy less than 16.6 eV [11]. The process is highly efficient, if the energy difference between the levels concerned is small [12].

The pressure p and the gas temperature T are assumed, respectively, to be 500 Torr and 300 K, consistent with the usual operation conditions of PDPs [6]. The ionization frequencies $\nu_{\rm Ne}$ and $\nu_{\rm Xe}$, as well as the electron drift velocity v_d, are calculated as a function of the reduced electric field E/N by numerically solving the full electron Boltzmann equation, using the Boltzmann code ELENDIF [13]. Electron–atom collision cross sections for Ne and Xe are taken from the SIGLO series [14], whereas $\gamma_{\rm Ne} = 0.5$ and $\gamma_{\rm Xe} = 0.05$ are taken from Meunier *et al.* [6]. It should be noted that in many cases, there is a lack of data concerning secondary electron emission coefficients and guessed values are often used in PDP models [6]. The results of

the models are sensitive to the uncertainties in these coefficients [10].

In the Ne–Xe case, the energy of the metastable atom is $\varepsilon_m \simeq 16.6$ eV, whereas the ionization energy of Xe is $[\varepsilon_i]_{\rm Xe} \simeq 12.1$ eV, so that the energy difference is approximately 4.5 eV. Penning ionization is represented by the reaction [15]

$$\mathrm{Ne}^m + \mathrm{Xe} \longrightarrow \mathrm{Ne} + \mathrm{Xe}^+ + e$$

where Ne and Ne^m represent a ground-state and metastable Ne atom, respectively, Xe and Xe^+ represent a ground-state Xe atom and its positive ion, respectively, and e is an electron.

The steady-state Townsend condition [16], [17] does not hold in typical PDP operation conditions, because the discharge is quickly quenched as a result of the accumulation of charge on the dielectric walls covering the electrodes, inducing a potential opposing the applied voltage. The duration of the discharge current pulse is on the order of $t_0 \simeq 10$ ns [6]. During this short time, the concentration of Ne metastable atoms N_{Ne^m} increases because of electron impact excitation and is determined by

$$\frac{dN_{\mathrm{Ne}^m}}{dt} = \nu_{\mathrm{Ne}^m} N_e - \nu^P_{\mathrm{Ne}^m} N_{\mathrm{Ne}^m}$$

where $\nu^P_{\mathrm{Ne}^m}$ is the Penning ionization frequency per Ne metastable atom and ν_{Ne^m} is the excitation frequency of the Ne metastable state. The average metastable atom concentration is therefore given as

$$\begin{aligned}\langle N_{\mathrm{Ne}^m}\rangle &= \frac{1}{t_0}\int_0^{t_0} N_{\mathrm{Ne}^m}(t)\,dt \\ &= \frac{\nu_{\mathrm{Ne}^m}}{\nu^P_{\mathrm{Ne}^m}}\left(1 + \frac{e^{-\nu^P_{\mathrm{Ne}^m} t_0} - 1}{\nu^P_{\mathrm{Ne}^m} t_0}\right) N_e\end{aligned}$$

where N_e is assumed to be constant during the discharge current pulse. Although this approximation is rough, it allows us to make a first-order estimate of N_{Ne^m}, and it provides a good estimate of the effect of Penning ionization. Our kinetic model results, as well as the 1-D simulations (Section IV), show that the Penning effect is not very significant in all three cases considered and, thus, results in relatively small changes in the breakdown field. Thus, possible inaccuracies in the calculation of Penning ionization do not have a significant effect on our results. The effective Penning ionization frequency per electron is then given as

$$\begin{aligned}[\nu^P_{\mathrm{Ne}^m}]_{\rm eff} &= \frac{\nu^P_{\mathrm{Ne}^m}\langle N_{\mathrm{Ne}^m}\rangle}{N_e} \\ &= \left(1 + \frac{e^{-\nu^P_{\mathrm{Ne}^m} t_0} - 1}{\nu^P_{\mathrm{Ne}^m} t_0}\right)\nu_{\mathrm{Ne}^m} \qquad (3)\end{aligned}$$

where we note that $\nu^P_{\mathrm{Ne}^m}$ is proportional to the concentration of Xe atoms. The corresponding effective partial first Townsend ionization coefficient is $\alpha_P = [\nu^P_{\mathrm{Ne}^m}]_{\rm eff}/v_d$. The frequency ν_{Ne^m} as a function of the reduced electric field E/N is calculated using the Boltzmann code [13], whereas $\nu^P_{\mathrm{Ne}^m}$ is taken from Levin *et al.* [15]. Stepwise ionization and recombination processes, as well as Penning ionization by collisions between two Xe excited atoms, are not taken into account in our modeling, because their effect on typical operational conditions for PDPs is negligible [6].

In the Ne–Xe case, the total excitation frequency ν^{tot}_{exc} is equal to the excitation frequency caused by electron collisions with Xe atoms ν_{exc}, because no other important excitation mechanisms exist [15]. The excitation frequency is, thus, calculated as a function of E/N using the Boltzmann code [13].

B. He–Xe Mixtures

In the He–Xe case, the self-sustaining condition for the calculation of the breakdown field is similar to the corresponding in the Ne–Xe case

$$\frac{\alpha_{\mathrm{He}}\gamma_{\mathrm{He}} + (\alpha_{\mathrm{Xe}} + \alpha_P)\gamma_{\mathrm{Xe}}}{\alpha_{\mathrm{He}} + \alpha_{\mathrm{Xe}} + \alpha_P}\left[e^{(\alpha_{\mathrm{He}} + \alpha_{\mathrm{Xe}} + \alpha_P)d} - 1\right] = 1 \quad (4)$$

where

- $\alpha_{\mathrm{He}} = \nu_{\mathrm{He}}/v_d$ partial first Townsend ionization coefficient for He;
- ν_{He} corresponding partial ionization frequency caused by direct ionization of neutral atoms by electrons;
- γ_{He} secondary electron emission coefficient for He ions on MgO;
- ν_{He} calculated as a function of E/N using the Boltzmann code [13].

Cross sections for He are taken from the SIGLO Series [14], whereas $\gamma_{\mathrm{He}} = 0.3$ is taken from Veerasingam *et al.* [18].

In the case of a He–Xe mixture, Penning ionization is represented by the reaction

$$\mathrm{He}^m + \mathrm{Xe} \longrightarrow \mathrm{He} + \mathrm{Xe}^+ + e$$

where He and He^m represent a ground-state and metastable He atom, respectively. In this case, the energy of the He metastable level is $\varepsilon_{\rm m} \simeq 20$ eV; so the energy difference with the Xe ionization level is approximately 7.9 eV. The effective Penning ionization frequency per electron is calculated in the same way as in the Ne–Xe case, and we obtain

$$[\nu^P_{\mathrm{He^m}}]_{\rm eff} = \left(1 + \frac{e^{-\nu^P_{\mathrm{He^m}} t_0} - 1}{\nu^P_{\mathrm{He^m}} t_0}\right)\nu_{\mathrm{He^m}} \qquad (5)$$

where

- $\nu_{\mathrm{He^m}}$ excitation frequency of the He metastable state;
- $\nu^P_{\mathrm{He^m}}$ Penning ionization frequency per He metastable atom taken from Rauf and Kushner [19];
- $\nu_{\mathrm{He^m}}$ calculated as a function of E/N using the Boltzmann code [13].

In addition, the total excitation frequency of the excited states of Xe that emit UV photons is equal to the excitation frequency caused by electron collisions with Xe atoms, because, as in the Ne–Xe case, no other important excitation mechanisms exist [19].

C. Ne–Xe–Ar Mixtures

In the case of the Ne–Xe–Ar mixture the breakdown field is calculated using the condition

$$\left[\frac{\alpha_{\rm Ne}\gamma_{\rm Ne}+(\alpha_{\rm Xe}+\alpha_{P1})\gamma_{\rm Xe}+(\alpha_{\rm Ar}+\alpha_{P2})\gamma_{\rm Ar}}{\alpha_{\rm Ne}+\alpha_{\rm Xe}+\alpha_{P1}+\alpha_{\rm Ar}+\alpha_{P2}}\right] \cdot\left[e^{(\alpha_{\rm Ne}+\alpha_{\rm Xe}+\alpha_{P1}+\alpha_{\rm Ar}+\alpha_{P2})d}-1\right]=1 \quad (6)$$

where

- $\alpha_{\rm Ar}=\nu_{\rm Ar}/v_d$ partial first Townsend ionization coefficient for Ar;
- $\nu_{\rm Ar}$ corresponding partial ionization frequency caused by direct ionization of argon atoms by electrons;
- $\gamma_{\rm Ar}$ secondary electron emission coefficient for Ar ions on MgO;
- $\nu_{\rm Ar}$ calculated as a function of E/N using the Boltzmann code [13].

Cross sections for Ar are taken from the SIGLO series [14], whereas $\gamma_{\rm Ar}=0.05$ is taken from Sahni *et al.* [7].

In this case, there are two Penning ionization reactions

$$\mathrm{Ne}^m+\mathrm{Xe}\longrightarrow \mathrm{Ne}+\mathrm{Xe}^+ +e \quad (7a)$$

$$\mathrm{Ne}^m+\mathrm{Ar}\longrightarrow \mathrm{Ne}+\mathrm{Ar}^+ +e \quad (7b)$$

where Ar and Ar^+ represent a ground-state Ar atom and its positive ion, respectively. In the second reaction, the argon ionization energy is $[\varepsilon_i]_{\rm Ar}\simeq 15.8$ eV; so the energy difference with the Ne metastable state is ~0.8 eV. Because the energy difference is small, this process is highly efficient [12]. The effective Penning ionization frequencies per electron are calculated in the same way as in the Ne–Xe and He–Xe case, and we obtain

$$\nu_{P1}=\frac{\nu_{i1}}{\nu_{i1}+\nu_{i2}}\left[1+\frac{e^{-(\nu_{i1}+\nu_{i2})t_0}-1}{(\nu_{i1}+\nu_{i2})t_0}\right]\nu_{\mathrm{Ne}^m} \quad (8a)$$

$$\nu_{P2}=\frac{\nu_{i2}}{\nu_{i1}+\nu_{i2}}\left[1+\frac{e^{-(\nu_{i1}+\nu_{i2})t_0}-1}{(\nu_{i1}+\nu_{i2})t_0}\right]\nu_{\mathrm{Ne}^m} \quad (8b)$$

where ν_{i1} and ν_{i2} are the Penning ionization frequencies per Ne metastable atom, corresponding to reactions (7a) and (7b). Note that ν_{i1} is the same quantity that was denoted as $\nu^P_{\mathrm{Ne}^m}$ in Section II-A, and it is taken from Levin *et al.* [15], whereas ν_{i2} has been taken from Sahni *et al.* [7]. The excited states of Xe that emit UV photons are mainly produced by electron impact reactions, as in the case of Ne–Xe and He–Xe mixtures. However, in this case, a particular excitation mechanism caused by collisions of Ar excited atoms with Xe atoms does exist

$$\mathrm{Ar}^*+\mathrm{Xe}\longrightarrow \mathrm{Ar}+\mathrm{Xe}^*$$

where Ar and Ar^* represent a ground-state and excited Ar atom, respectively, and Xe and Xe^* represents a ground-state and excited Xe atom, respectively [20]. In the Ne–Xe–Ar mixtures under consideration, this reaction is the dominant loss mechanism of Ar excited atoms. Thus, the total excitation frequency of the excited states of Xe that emit UV photons ν^{tot}_{exc} is equal to the direct excitation frequency $\nu^{\rm Xe}_{exc}$ caused by electron collisions with Xe atoms plus the excitation frequency $\nu^{\rm Ar}_{exc}$ caused by electron collisions with Ar atoms. Both $\nu^{\rm Xe}_{exc}$ and $\nu^{\rm Ar}_{exc}$ are calculated as a function of E/N using the Boltzmann code [13].

III. Results

Our stated goal in this paper is to compare the different gas mixtures by their breakdown voltage and efficiency defined as the ratio of the energy spent in excitation of UV emitting states of Xe per unit volume and per unit time, over the dissipated power per unit volume. However, the electric field E in the PDP cell during the discharge is spatially nonuniform because of space charges, with its spatial distribution being time dependent. In addition, Xe excitation, which has a highly nonlinear dependence on the electric field, occurs both in the high- and low-field regions. Accordingly, we evaluate the efficiency η for $E=0.2E_k,\ E_k,\ 5E_k$, where E_k is the breakdown field for our conditions ($p=500$ Torr, $T=300$ K) calculated using (2), (4), and (6) in the case of Ne–Xe, He–Xe, and Ne–Xe–Ar mixtures, respectively. This range of electric field values, defined with respect to E_k, encompasses electric fields typically encountered in PDP cells, according to previous 1-D or two-dimensional (2-D) models [6].

In the following subsections, we separately examine each of the three gas mixtures.

A. Ne–Xe Mixtures

Fig. 2(a) shows the variation of the breakdown gap voltage $V_g\equiv E_k d$ as a function of the Xe concentration $N_{\rm Xe}$ in the mixture, calculated using (2). We observe that for $N_{\rm Xe}\geq 0.02N$, E_k is an increasing function of $N_{\rm Xe}$. The Penning effect is found to not be significant for this mixture, because $[\nu^P_{\mathrm{Ne}^m}]_{\rm eff}$ is found to be less than ~12% of the total ionization frequency ν^{tot}_{ion} for the full range of parameter values. Fig. 2(b) shows the excitation frequency ν_{exc} as a function of $N_{\rm Xe}$ for $E=0.2E_k,\ E_k,\ 5E_k$, keeping in mind that E_k is also a function of the concentrations of the constituent gases. We observe that for small values of $N_{\rm Xe}$, ν_{exc} increases dramatically with small percentage increases in Xe concentration, whereas ν_{exc} increases at a much smaller rate for high Xe concentrations. We also observe that $\nu_{exc}(0.2E_k)\ll\nu_{exc}(E_k)\ll\nu_{exc}(5E_k)$, independent of $N_{\rm Xe}$, because at higher E, electron impact excitation reactions are more efficient. Fig. 2(c) shows the efficiency η as a function of $N_{\rm Xe}$, calculated in the way described above. We observe that the discharge is more efficient at low electric field values, although the number of UV photons emitted is higher at high electric field values [Fig. 2(b)]. Efficiency is also an increasing function of $N_{\rm Xe}$.

The numerical results given in Fig. 2 can be interpreted by the inherent kinetic behavior of Ne and Xe under applied electric fields. Fig. 2(d) shows the dynamic friction force of electrons, also known as the electron energy loss function, as a function of electron energy in a pure Ne gas, a pure Xe gas, and a 10% Xe–90% Ne gas mixture. In any given mixture, the loss function is defined as

$$F(\varepsilon)=\sum_i N_i\sigma_i(\varepsilon)\delta\varepsilon_i,$$

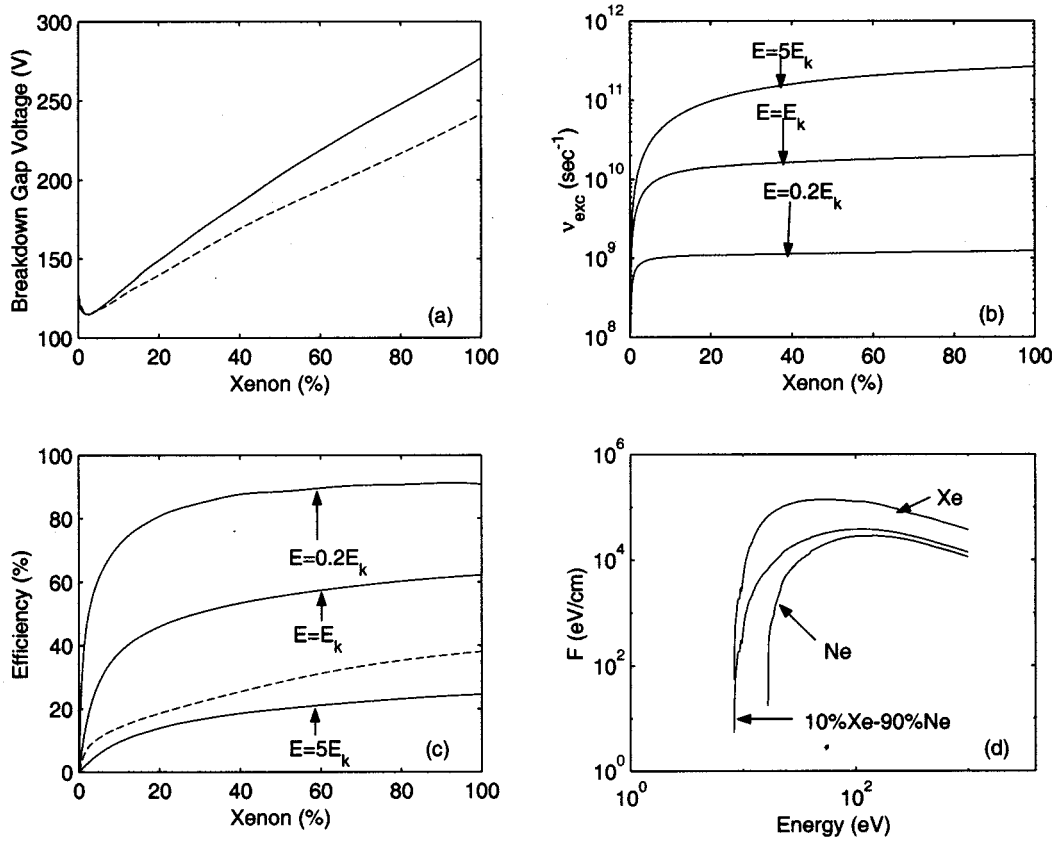

Fig. 2. (a) Breakdown gap voltage as a function of Xe concentration $N_{\rm Xe}$ in Ne–Xe mixtures, calculated using (2). The dashed line shows the mid-margin gap voltage, calculated using the 1-D model. (b) Excitation frequency ν_{exc} as a function of $N_{\rm Xe}$. (c) Efficiency (%) η as a function of $N_{\rm Xe}$. The dashed line shows the efficiency of the discharge, calculated using the 1-D model. (d) The loss function as a function of electron energy in a pure Ne gas, a pure Xe gas, and a 10% Xe–90% Ne gas mixture.

where the summation is over of all the collision cross sections of inelastic processes σ_i with corresponding energy loss $\delta\varepsilon_i$, and N_i is the number density of the corresponding target atoms. The dynamic friction force has units electronvolts/meters (energy loss per unit length), and it can be thought of as an effective force acting on electrons against the accelerating action of the electric field.

The breakdown field is much higher for Xe compared with Ne, as is evident from Fig. 2(a). That this is the case can be understood in terms of the corresponding loss functions. The ionization energy of Xe is $[\varepsilon_i]_{\rm Xe} \simeq 12.1$ eV, wheras $[\varepsilon_i]_{\rm Ne} \simeq 21.6$ eV. However, the dynamic friction for Xe is much higher than that for Ne, because the excitation and ionization cross sections of Xe are almost one order of magnitude higher [14] than are those of Ne. Thus, if the same electric field is applied at a pure Xe versus a pure Ne gas, the number of electrons above the corresponding ionization threshold is much higher in Ne, accounting for the fact that E_k is an increasing function of $N_{\rm Xe}$ [Fig. 2(a)] in Ne–Xe mixtures. This is also because the secondary electron emission coefficient $\gamma_{\rm Ne}$ for neon ions on MgO is an order of magnitude higher than is the corresponding coefficient $\gamma_{\rm Xe}$ for xenon ions. The loss function (or dynamic friction) also determines the electron energy distribution function that is attained in a gas for a given applied electric field. For small values of $N_{\rm Xe}$, the loss function (and, thus, the electron energy distribution) does not vary significantly with increasing $N_{\rm Xe}$, so that the dynamic friction at the excitation energy of Xe is relatively low, and many electrons have energies above this threshold, leading to the dramatic increase of Xe excitation frequency ν_{exc}. The corresponding partial ionization frequency of Xe (i.e., $\nu_{\rm Xe}$) increases dramatically for the same reason, whereas the corresponding partial ionization frequency $\nu_{\rm Ne}$ of Ne slightly decreases, because the electron distribution function is only slightly perturbed by the addition of a small amount of Xe in Ne. Thus, E_k is a decreasing function of $N_{\rm Xe}$ for small $N_{\rm Xe}$ ($N_{\rm Xe} \leq 0.02\,N$).

The results presented in Fig. 2(a) and (c) should allow quantitative evaluation of the effects of Xe percentage in Ne–Xe mixtures in practice. In this context, it is desirable to have high luminous efficiency and low breakdown field (i.e., lower voltage operation). From Fig. 2(c), we note that although η increases rapidly with Xe percentage for low values of $N_{\rm Xe}$, the rate of increase in η decreases with increasing $N_{\rm Xe}$. Specifically, we note that although $\eta \simeq 70\%$ for $N_{\rm Xe} \simeq 0.1\,N$, it is only $\sim$10% higher for $N_{\rm Xe} \simeq 0.2\,N$, whereas the breakdown voltage is $\sim$25% higher. In Section IV, we show that the dependence of the actual discharge efficiency on $N_{\rm Xe}$ is very similar.

B. He–Xe Mixtures

Fig. 3(a) shows the breakdown gap voltage $V_g \equiv E_k d$ as a function of Xe concentration $N_{\rm Xe}$ in a He–Xe mixture, calculated using (4). The functional dependence of E_k on $N_{\rm Xe}$ is

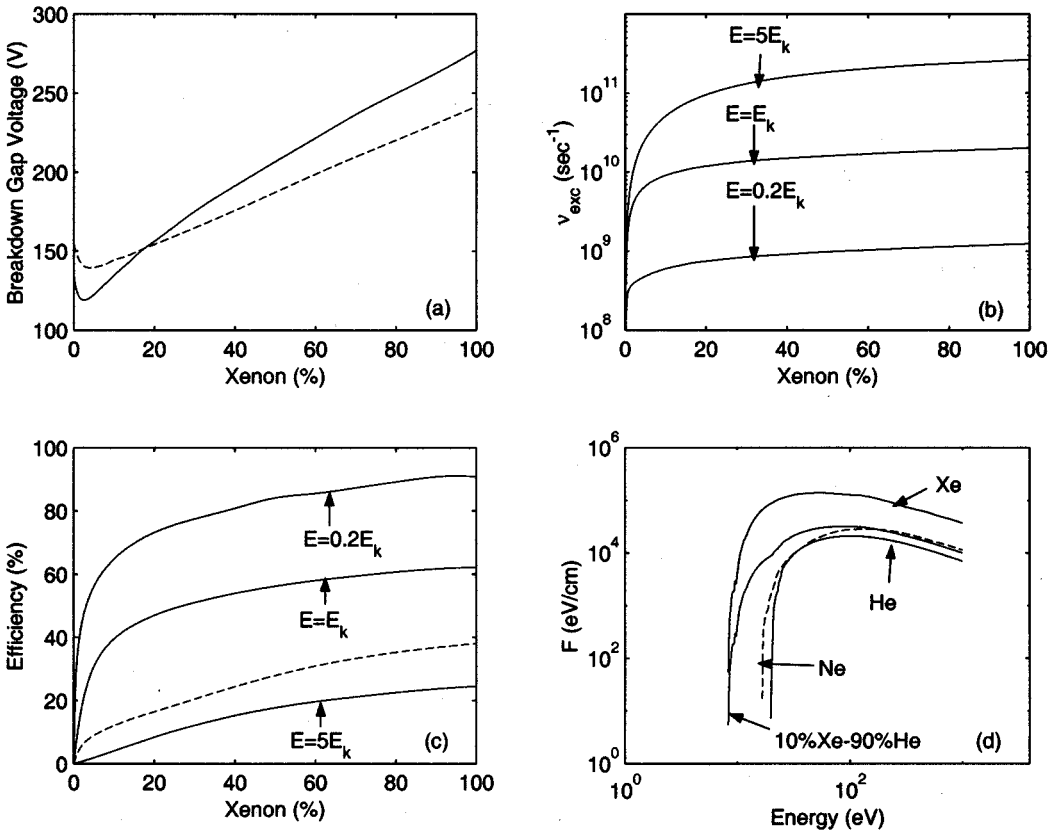

Fig. 3. (a) Breakdown gap voltage as a function of $N_{\rm Xe}$ in He–Xe mixtures, calculated using (4). The dashed line shows the mid-margin gap voltage, calculated using the 1-D model. (b) Excitation frequency ν_{exc} as a function of $N_{\rm Xe}$. (c) Efficiency (%) η as a function of $N_{\rm Xe}$. The dashed line shows the efficiency of the discharge, calculated using the 1-D model. (d) The loss function as a function of electron energy in a pure He gas, a pure Ne gas (dashed line), a pure Xe gas, and a 10% Xe–90% He gas mixture.

similar to the Ne–Xe case. However, E_k is slightly higher in a He–Xe mixture compared with a Ne–Xe mixture with the same Xe concentration. The contribution of the Penning effect is also not significant for this case, because $[\nu^P_{\rm He^m}]_{\rm eff}$ is found to be less than $\sim$7% of ν^{tot}_{ion} for the full range of parameter values considered. Fig. 3(b) shows the excitation frequency ν_{exc} of Xe as a function of $N_{\rm Xe}$ for $E = 0.2E_k$, E_k, $5E_k$. The results are similar to the Ne–Xe case, although ν_{exc} values are smaller. Because of the higher breakdown field and the smaller Xe excitation frequency, the efficiency is smaller, as shown in Fig. 3(c). However, it should be noted that He–Xe mixtures achieve better color purity, because the discharge does not produce visible light as in the Ne–Xe case [8].

In Fig. 3(d), we plot the loss function as a function of electron energy in a pure He gas, a pure Xe gas, and a 10% Xe–90% He gas mixture. For comparison, we also plot the loss function for pure Ne. We observe that the loss function for pure Ne has slightly higher values than that for pure He. Based on the discussion in Section III-A, we would expect slightly lower ionization and excitation frequencies in Ne–Xe mixtures in comparison with He–Xe mixtures. However, the ionization and excitation frequencies in He–Xe mixtures are actually lower compared with Ne–Xe mixtures with the same Xe concentration, resulting in higher breakdown field and lower efficiency. It was found that this unexpected result is mainly caused by the higher electron momentum transfer cross section of He compared with that of Ne [14]. Because the loss functions are almost equal, this effect dominates, resulting in lower ionization and excitation frequencies in He–Xe mixtures in comparison with Ne–Xe mixtures with the same Xe concentration [21]. The higher breakdown field in He–Xe mixtures is also because of the lower secondary electron emission coefficient $\gamma_{\rm He}$ of helium ions on MgO, compared with the coefficient $\gamma_{\rm Ne}$ of neon ions.

From a practical point of view, we note from Fig. 3(a) and (c) that the tradeoff between luminous efficiency and breakdown voltage level is similar for He–Xe mixtures as for Ne–Xe mixtures.

C. Ne–Xe–Ar Mixtures

In Section III-A, we saw that for Ne–Xe mixtures, the efficiency η is an increasing function of $N_{\rm Xe}$. However, the breakdown field E_k is also an increasing function of $N_{\rm Xe}$. In addition, in Section III-B, we saw that Ne–Xe mixtures are more efficient than are He–Xe mixtures. In this section, we investigate the effect of adding a small amount of Ar in Ne–Xe mixtures, as is done in some PDP designs.

Fig. 4(a) shows $V_g \equiv E_k d$ as a function of Ar concentration $N_{\rm Ar}$ in a mixture with $N_{\rm Xe}/N_{\rm Ne} = 5/95$. We observe that E_k decreases when small amounts of Ar are added, caused primarily by the Penning ionization reaction of Ar atoms with Ne metastable atoms, as described in (7b). By examination of

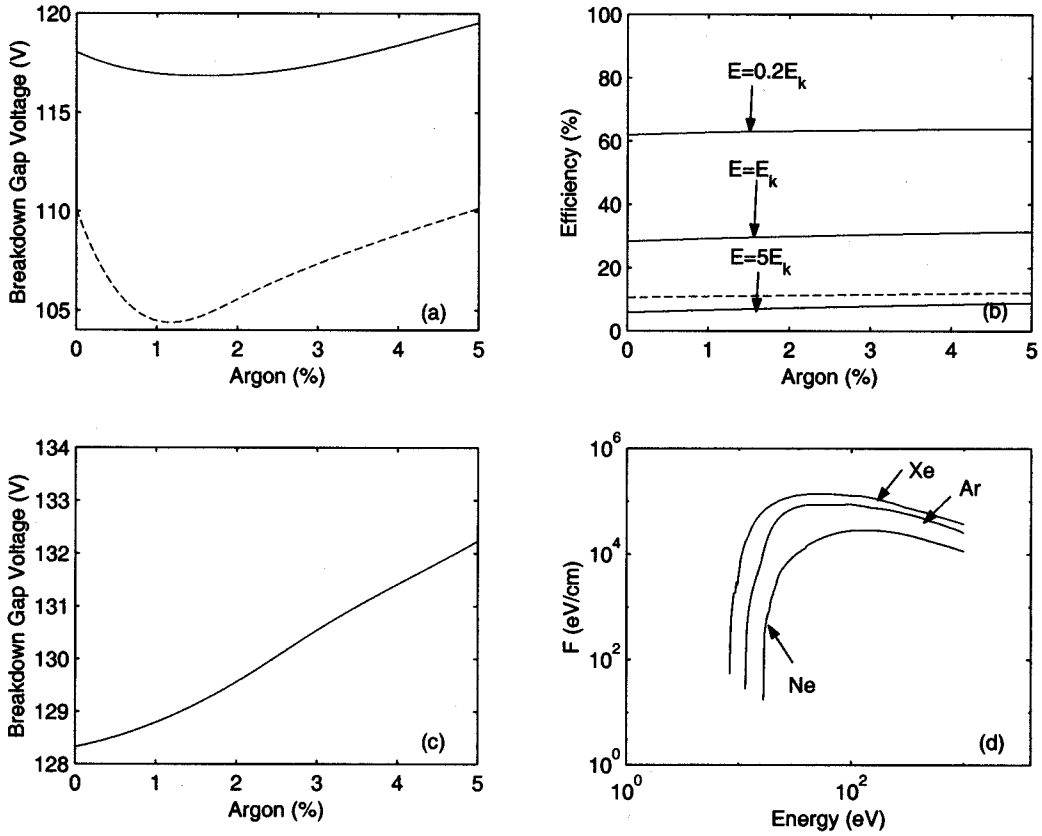

Fig. 4. (a) Breakdown gap voltage as a function of Ar concentration $N_{\rm Ar}$ in a mixture with $N_{\rm Xe}/N_{\rm Ne} = 5/95$, calculated using (6). The dashed line shows the mid-margin gap voltage, calculated using the 1-D model. (b) Efficiency (%) η as a function of $N_{\rm Ar}$ in a mixture with $N_{\rm Xe}/N_{\rm Ne} = 5/95$. The dashed line shows the efficiency of the discharge, calculated using the 1-D model. (c) Breakdown gap voltage as a function of $N_{\rm Ar}$ in a mixture with $N_{\rm Xe}/N_{\rm Ne} = 10/90$, calculated using (6). (d) The loss function as a function of electron energy in a pure Ne gas, a pure Xe gas, and a pure Ar gas.

the loss functions of Ne, Ar, and Xe, plotted in Fig. 4(d), we observe that the friction losses are higher in Ar than in Ne. Thus, when Ar is added to the mixture, the dynamic friction force on electrons increases, and we would ordinarily expect to see a corresponding increase in E_k. However, E_k actually decreases because of Penning ionization of Ar atoms by Ne metastables, which is very efficient, as mentioned above. We note from Fig. 4(a) that E_k is minimized at $N_{\rm Ar} \simeq 0.01\,N$. For $N_{\rm Ar} > 0.01\,N$ the increased losses dominate over the Penning ionization effect and E_k increases. Fig. 4(b) shows the luminous efficiency of the gas mixture as a function of $N_{\rm Ar}$. The efficiency slightly increases when small amounts of Ar are added. Thus, adding a small amount of Ar to a Ne–Xe mixture both decreases E_k and increases η. However, both of these improvements are relatively small, being less than $\sim$1%.

Fig. 4(c) shows $V_g \equiv E_k d$ as a function of $N_{\rm Ar}$ in a mixture with $N_{\rm Xe}/N_{\rm Ne} = 10/90$. The Penning effect is less important in comparison with the previous case because of the higher Xe concentration. As a result, the effect of the increased losses dominates and E_k increases when small quantities of Ar are added to the mixture.

Based on the results shown in Fig. 4, there does not seem to be any significant advantage in using small amounts of Ar in Ne–Xe mixtures, at least from the point of view of fundamental properties of the gases.

IV. Comparison with 1-D Simulation Results

In order to assess the validity of conclusions derived from our fundamental kinetic analysis of unbounded and homogeneous gas mixtures, we have developed a 1-D self-consistent simulation of an ac PDP cell, similar to those previously developed by Meunier *et al.* [6] and Punset *et al.* [22]. The space and time variation of the electric field within the gas is self-consistently determined by solving the fluid equations for ions and electrons together with Poisson's equation, subject to the boundary conditions imposed by the electrode boundaries. Ionization caused by Penning reactions is also included. The data used in the 1-D model, such as electron–atom collision cross sections, secondary electron emission coefficients, and reaction rates are identical to those used in the homogeneous and unbounded kinetic model. The gap length d, the pressure p, and the gas temperature T are also chosen to be the same as in the unbounded model. Other model parameters, such as length and relative permittivity of dielectrics, are identical to those used in Meunier *et al.* [6].

We use the 1-D model to calculate the voltage margin of stable operation of the cell by the voltage transfer curve method, introduced by Slottow and Petty [5] and described in Meunier *et al.* [6]. In each case, we use an applied voltage corresponding to operation in the middle of the calculated voltage margin to determine the efficiency of the discharge. The energy dissipated

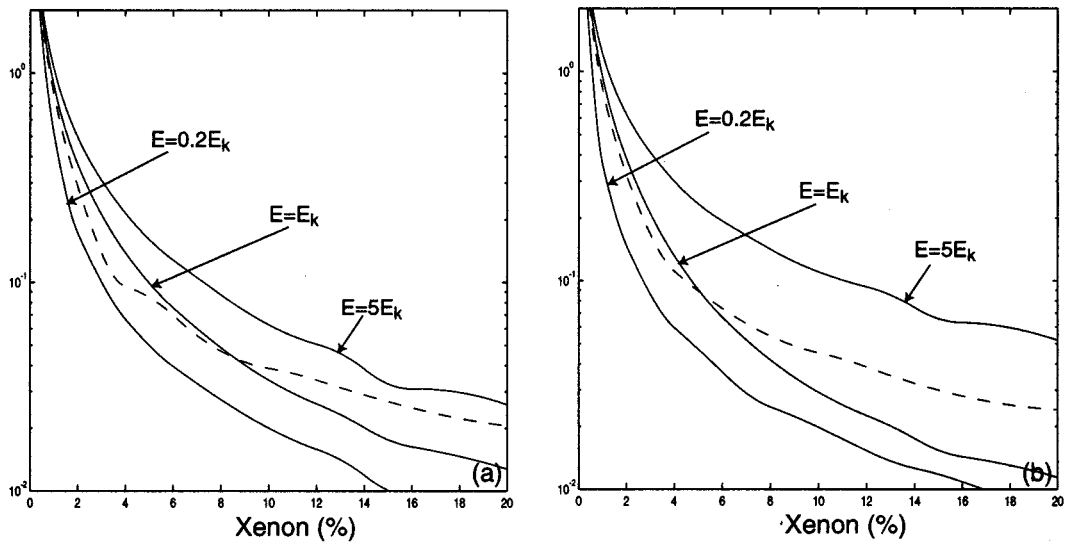

Fig. 5. (a) Normalized derivative of the efficiency η as a function of $N_{\rm Xe}$ in Ne–Xe mixtures. The dashed line shows the normalized derivative of the efficiency of the discharge, calculated using the 1-D model. (b) Normalized derivative of the efficiency η as a function of $N_{\rm Xe}$ in He–Xe mixtures. The dashed line shows the normalized derivative of the efficiency of the discharge, calculated using the 1-D model.

by electrons and ions, as well as the energy spent in excitation of UV emitting states of Xe are calculated. In other words, efficiency η is calculated as given by (1), except for the fact that $P_{diss} = E(J_e + J_{ion}) = (N_e q_e \mu_e + \sum_i N_i q_i \mu_i)E^2$.

The dashed line curve in Fig. 2(a) shows the variation of the mid-margin sustaining voltage in the gap V_{sg} as a function of the Xe concentration $N_{\rm Xe}$ in a Ne–Xe mixture. V_{sg} is given by

$$V_{sg} = \left[\frac{C_D}{C_D + C_g}\right] \frac{V_s^{\min} + V_s^{\max}}{2}$$

where

C_D equivalent capacitance of the dielectric layers;

C_g gas gap capacitance;

$V_s^{\min}$, $V_s^{\max}$ calculated minimum and maximum values of the sustaining voltage.

The dashed curve in Fig. 2(c) shows the variation of the discharge efficiency as a function of $N_{\rm Xe}$ in Ne–Xe mixtures for a middle-margin applied sustaining voltage. These 1-D results show that the sustaining voltage and the discharge efficiency of the PDP cell exhibit very similar dependence on $N_{\rm Xe}$ with the corresponding quantities of the unbounded homogeneous kinetic model. This similarity is further illustrated in Fig. 5(a), where we show the normalized derivative of the efficiency ($\eta^{-1} d\eta/d[N_{\rm Xe}/N]$) as a function of $N_{\rm Xe}$. The dashed line curve shows the normalized derivative of the discharge efficiency, calculated with the 1-D simulation. This plot illustrates that the fractional increase in η is very small for $N_{\rm Xe} > 0.1\,N$. It also illustrates that the dependence of the discharge efficiency on $N_{\rm Xe}$ is determined by the fundamental property η of the gas mixture.

The dashed lines in Figs. 3(a), 3(c), and Fig. 5(b) show similar results for He–Xe mixtures. In agreement with the unbounded and homogeneous kinetic model, it is found that V_{sg} is higher in a He–Xe mixture compared with a Ne–Xe mixture with the same Xe concentration and that the discharge efficiency is lower. It should be noted that He exhibits a very gradual rise in the slope of the voltage transfer curve [18]. We found that this is mainly from the high electron momentum transfer cross section of He. In agreement with Veeresingam *et al.* [18], we found that this effect results in disagreement between the actual $V_s^{\min}$, $V_s^{\max}$ and those calculated using the voltage transfer curve method for He–Xe mixtures with high helium concentrations. However, in the discharge efficiency calculation, we used an applied sustaining voltage that results in a stable discharge.

The dashed curves in Fig. 4(a) and (b) show V_{sg} and discharge efficiency as a function of Ar concentration $N_{\rm Ar}$ in a mixture with $N_{\rm Xe}/N_{\rm Ne} = 5/95$. In agreement with the results of the unbounded homogeneous model, V_{sg} is minimized at $N_{\rm Ar} \simeq 0.01\,N$ because of Penning ionization, and the efficiency slightly increases when small amounts of Ar are added. Although these improvements of $\sim$5% seem to have been underestimated by the unbounded homogeneous model, they are still small, confirming that there is no significant advantage in using small amounts of Ar in Ne–Xe mixtures.

V. Summary

We have considered the fundamental kinetic behavior under an applied electric field of homogeneous, unbounded inert gas mixtures to compare the breakdown field and UV photon generation efficiency of Ne–Xe, He–Xe, and Ne–Xe–Ar mixtures used in PDPs. Efficiency is an increasing function of Xe concentration in Ne–Xe and He–Xe mixtures, although He–Xe mixtures were found to be less efficient than were Ne–Xe mixtures with the same Xe concentration. The fractional increase in efficiency is very small for $N_{\rm Xe} > 0.1\,N$.

For Ne–Xe mixtures with $N_{\rm Xe}/N_{\rm Ne} = 5/95$, the addition of a small amount of Ar results in a slight minimum in the breakdown field at $N_{\rm Ar}/N \simeq 0.01$, whereas the efficiency increases only slightly. For Ne–Xe mixtures with $N_{\rm Xe}/N_{\rm Ne} = 10/90$, the addition of a small amount of Ar increases the breakdown

field. Based on these results, the addition of Ar to Ne–Xe mixtures does not lead to any significant improvement in PDP performance, either in terms of luminous efficiency or breakdown voltage level.

Using a 1-D model of an ac PDP cell, we confirmed the validity of the conclusions derived by the homogeneous and unbounded kinetic model.

REFERENCES

[1] A. Sobel, "Television's bright new technology," *Sci. Am.*, vol. 278, pp. 70–77, May 1998.

[2] S. Matsumoto, *Electronic Display Devices*. New York: Wiley, 1990, p. 131.

[3] Y. Sano, T. Nakamura, K. Numomura, T. Konishi, M. Usui, A. Tanaka, T. Yoshida, H. Yamada, O. Oida, and R. Fujimura, "High-contrast 50-in. color ac plasma display with 1365 × 768 pixels," *SID'98 Dig.*, pp. 275–278, 1998.

[4] H. Hirakawa, T. Katayama, S. Kuroki, T. Kanae, H. Nakahara, T. Nanto, K. Yoshikawa, A. Otsuka, and M. Wakitani, "Cell structure and driving method of a 25-in. (64-cm) diagonal high-resolution color ac plasma display," *SID'98 Dig.*, pp. 279–282, 1998.

[5] H. G. Slottow and W. D. Petty, "Stability of discharge series in the plasma display panel," *IEEE Trans. Electron Devices*, vol. ED-18, pp. 650–654, Sept. 1971.

[6] J. Meunier, Ph. Belenguer, and J. P. Boeuf, "Numerical model of an ac plasma display panel cell in neon-xenon mixtures," *J. Appl. Phys.*, vol. 78, pp. 731–745, July 1995.

[7] O. Sahni, C. Lanza, and W. E. Howard, "One-dimensional numerical simulation of ac discharges in a high-pressure mixture of Ne+0.1% Ar confined to a narrow gap between insulated metal electrodes," *J. Appl. Phys.*, vol. 49, pp. 2365–2375, Apr. 1978.

[8] M. Noborio, T. Yoshioka, Y. Sano, and K. Nunomura, "(He,Ne)–Xe gas mixtures for high-luminance color ac PDP," *SID'94 Dig.*, pp. 727–730, 1994.

[9] F. M. Penning, *Electrical Discharges in Gases*. New York: MacMillan , 1957, p. 29.

[10] J. P. Boeuf, C. Punset, and H. Doyeux, "Physics and modeling of plasma display panels," *J. Phys. IV*, vol. 7, pp. 3–14, Oct. 1997.

[11] F. M. Penning, *Electrical Discharges in Gases*. New York: Macmillan , 1957, p. 15.

[12] J. M. Meek and J. D. Craggs, *Electrical Breakdown of Gases*. New York: Wiley, 1978, p. 68.

[13] W. L. Morgan and B. M. Penetrate, "ELENDIF: A time-dependent Boltzmann solver for partially ionized plasmas," *Comput. Phys. Commun.*, vol. 58, pp. 127–152, 1990.

[14] [Online]http://www.sni.net/siglo/database/xsect/siglo.sec

[15] L. A. Levin, S. E. Moody, E. L. Klosterman, R. E. Center, and J. J. Ewing, "Kinetic model for long-pulse XeCl laser performance," *IEEE J. Quantum Electron.*, vol. QE-17, pp. 2282–2289, Dec. 1981.

[16] Y. Sakai, S. Sawada, and H. Tagashira, "Boltzmann equation analyzes of electron swarm parameters in Ar/Ne, Kr/Ne, Xe/Ne, Hg/Ar and Hg/Kr mixtures and derived effective excitation cross sections for metastable states of rare atoms," *J. Phys. D: Appl. Phys.*, vol. 24, pp. 283–289, 1991.

[17] F. M. Penning, "The starting potential of the glow discharge in neon argon mixtures between large parallel plates," *Physica*, vol. 1, pp. 1028–1044, 1934.

[18] R. Veerasingam, R. B. Campbell, and R. T. McGrath, "One-dimensional single and multipulse simulations of the ON/OFF voltages and the bistable margin for He, Xe, and He/Xe filled plasma display pixels," *IEEE Trans. Plasma Sci.*, vol. 24, pp. 1399–1410, Dec. 1996.

[19] S. Rauf and M. J. Kushner, "Dynamics of a coplanar-electrode plasma display panel cell. I. Basic operation," *J. Appl. Phys.*, vol. 85, no. 7, pp. 3460–3469, Apr. 1999.

[20] F. Kannari, A. Suda, M. Obara, and T. Fujioka, "Theoretical simulation of electron-beam-excited xenonchloride (XeCl) lasers," *IEEE J. Quantum Electron.*, vol. QE-19, pp. 1587–1600, Oct. 1983.

[21] S. Rauf and M. J. Kushner, "Dynamics of a coplanar-electrode plasma display panel cell. II. Cell optimization," *J. Appl. Phys.*, vol. 85, pp. 3470–3476, Apr. 1999.

[22] C. Punset, J. P. Boeuf, and L. C. Pitchford, "Two-dimensional simulation of an alternating current matrix plasma display cell: Cross-talk and other geometric effects," *J. Appl. Phys.*, vol. 83, pp. 1884–1897, Feb. 1998.

Georgios Veronis was born in Greece on January 11, 1975. He received the B.S. degree from the National Technical University of Athens, Greece, in 1997 and the M.S. degree from Stanford University, Stanford, CA, in 1999, in electrical engineering. Since 1997, he has been a Research Assistant in the Space, Telecommunications, and Radioscience (STAR) Laboratory at Stanford University, where he is pursuing the Ph.D. degree. His research interests include plasma physics and applications, and computational electromagnetics.

Umran S. Inan (S'76–M'82–SM'99) was born in Turkey on December 28, 1950. He received the B.S. and M.S. degrees in electrical engineering from the Middle East Technical University in Ankara, Turkey in 1972 and 1973, respectively, and his Ph.D. degree in electrical engineering from Stanford University in 1977. He is currently a Professor of electrical engineering at Stanford University, where he serves as Director of the Space, Telecommunications, and Radioscience (STAR) Laboratory. He has received the 1998 Stanford University Tau Beta Pi Award for Excellence in Undergraduate Teaching, and actively conducts research in electromagnetic waves in plasmas, lightning discharges, ionospheric physics, and very low frequency remote sensing. Dr. Inan has served as the Ph.D. thesis adviser for 13 students and is a member of Tau Beta Pi, Sigma Xi, the American Geophysical Union, the Electromagnetics Academy, and currently serves as Secretary of US National Committee of the International Union of Radio Science (URSI).

Victor P. Pasko received his undergraduate and Candidate of Sciences degrees in theoretical physics and mathematics from Kiev University, Ukraine, in 1987 and 1990, respectively. He received his Ph.D. degree in electrical engineering from Stanford University in 1996. Dr. Pasko is currently an Engineering Research Associate in the Department of Electrical Engineering of Stanford University.

Dr. Pasko has published 32 peer-reviewed scholarly articles dealing with the theory of strong shock wave propagation in the interstellar medium, kinetic theory of collisionless electron beam-plasma relaxation with applications to active experiments in space, linear, and nonlinear theories of plasma stratification in cometary tails and in the auroral region, relaxation of transient lower ionospheric disturbances caused by lightning-whistler-induced electron precipitation, the nonlinear coupling of quasielectrostatic thundercloud fields to the mesosphere and lower ionosphere, diffraction effects of gravity waves generated by tropospheric convection, upward mapping and heating effects of electrostatic thundercloud fields, dynamics and spectroscopy of different types of electrical breakdown in air, and ELF radiation from sprites. He has reported his work in over 50 talks at national and international meetings. In 1996 Dr. Pasko was awarded an NSF (CEDAR) Post-Doctoral Award.

In 1996, he also received the Young Scientist Award of International Union of Radio Science (URSI). Dr. Pasko is a member of the American Geophysical Union and U.S. Comission H of URSI.